PROC. 15TH INT. CONF. PHYSICS OF SEMICONDUCTORS, KYOTO, 1980
J. PHYS. SOC. JAPAN **49** (1980) SUPPL. A p. 1271–1280

CRYSTAL GROWTH AND IMPURITY INCORPORATION BY TRANSIENT LASER AND ELECTRON BEAM HEATING OF SEMICONDUCTORS

W. L. Brown

Bell Laboratories
Murray Hill, New Jersey 07974

The transient heating of semiconductors by lasers or electron beams has extended studies of crystal growth and impurity incorporation into new regions of growth velocity and incorporated impurity concentration. Such directed energy beams have also enabled the study of crystal growth on non-crystalline substrates and provided new means for studying the thermodynamic properties of amorphous semiconductors.

I. Introduction

It is widely but not universally accepted that the principle response of a semiconductor to nanosec pulses from lasers or electron beams can be understood in terms of melting and refreezing a thin layer at the surface [1]. The initial excitation of the material is, of course, in the electronic system with the formation of free carriers; that excitation is rapidly transferred to atomic motion (heat) on time scales of nanosecs or less [2,3].

The coupling of laser energy into the material is strongly influenced by the wavelength of light, the temperature, and the carrier concentration, impurity, defect structure and phase (amorphous, crystalline, or liquid) of the semiconductor [2]. There often are major changes in the coupling during a pulse due to changes in free carrier absorption [4], band gap narrowing and melting. The coupling of keV pulsed electron energy into a material is essentially independent of the subleties of the material properties, even its phase, since the primary excitations involve a wide variety of states not near the band edge [2].

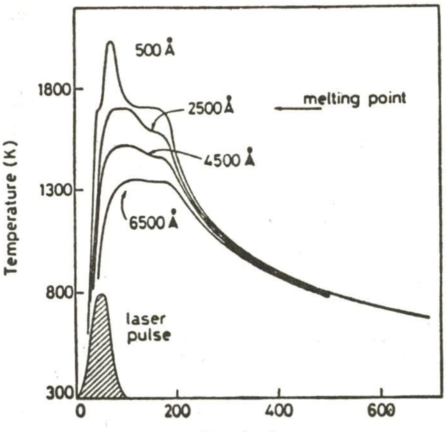

Fig. 1 Calculation due to Baeri of the time dependence of temperature at different depths in silicon during and following a 50 nsec. ruby laser pulse [5]

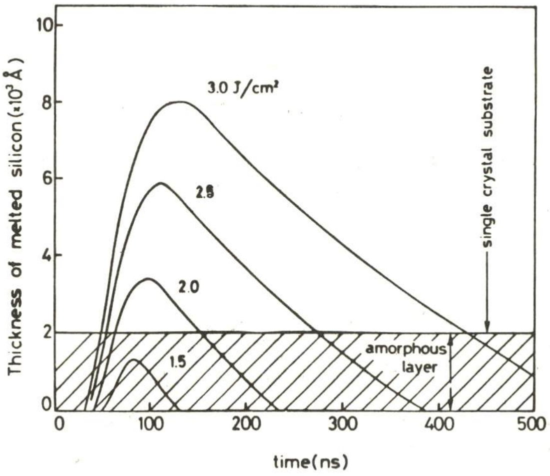

Fig. 2 Calculation due to Baeri of the melt layer thickness in silicon as a function of time due to 50 nsec. ruby laser pulses of different energy density [5].

Figure (1), due to Baeri et al [5], illustrates the calculated temperature verses time at several depths in silicon during and following a 50 nsec ruby laser pulse. The maximum depth of melting depends on the laser energy. In this case a layer slightly thicker than 2500Å is transiently melted and refrozen. The thermal conduction of the material plays a very important role in the time development by carrying heat rapidly into the bulk of the material. It is convenient to think of the advance and retreat of a molten zone as shown in Figure (2). A 2000Å amorphous layer is assumed to exist initially at the surface. At a low enough laser energy the molten zone will not encompass the whole of this layer and when refreezing occurs the silicon will regrow polycrystalline since it has no crystalline template to organize its long range order. When melting penetrates into the underlying crystal, however, single crystal material is formed on regrowth. The time to refreeze the whole layer as well as the velocity of regrowth is dependent on the energy of the exciting pulse. Note the times are the order of 100's of nsec.

The depth distribution of implanted impurities is strongly influenced by the molten zone as shown in Figure (3), the distribution of arsenic determined from Rutherford backscattering in silicon that has been laser annealed with 75 nsec 1.06 micron Nd:YAG pulses at several different powers [6]. Broader arsenic depth distributions are found for higher power pulses. This is understood as due to diffusion of arsenic in the liquid phase. Higher powers give thicker liquid layers and longer times for this diffusion, in general agreement with liquid diffusivities for arsenic $\approx 10^{-4}$cm^2/sec. This point will be discussed further in a Section IV.

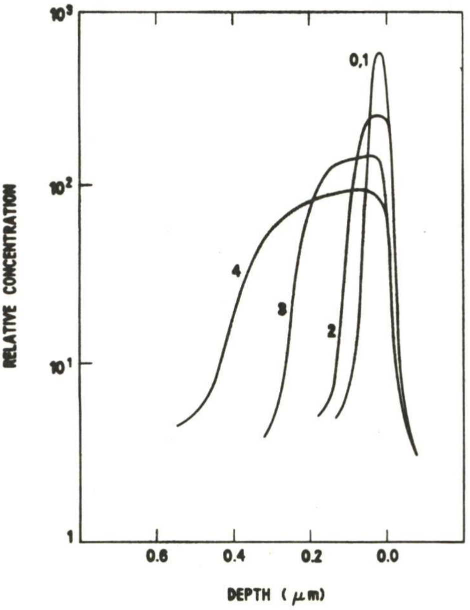

Fig. 3 Measured arsenic depth profiles before and following 75 nsec Nd:YAG 1.06μ pulses of different energy density [6]: 0=before laser pulsing; 1=43MWcm^{-2}; 2=62MWcm^{-2}; 3=84MWcm^{-2}; 4=105MWcm^{-2}

II. Threshold Measurements of the Thermodynamic Properties of Amorphous Silicon

Figure 4, due to Bagley and Chen [7], shows the free energy of a typical semiconductor in amorphous and crystalline states. The amorphous state is disordered and can spontaneously transform to the

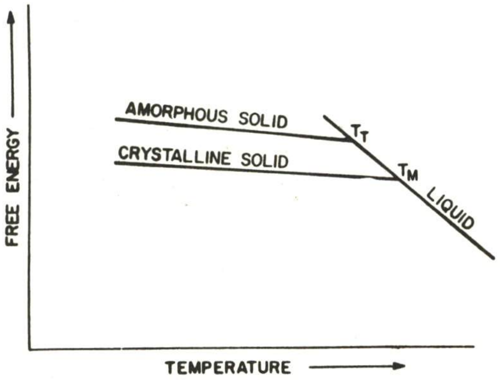

Fig. 4 Schematic free energy diagram for amorphous and crystalline semiconductor [7]

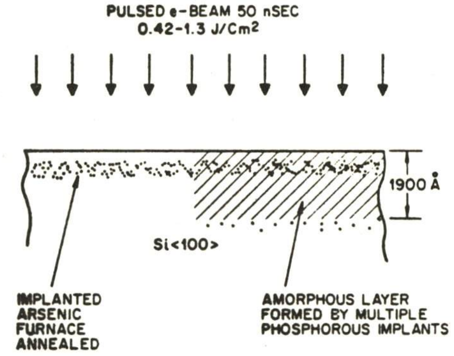

Fig. 5 Schematic cross section illustrating the experiment of Baeri et al [9] to measure the thermodynamic properties of amorphous Si: The arsenic layer is a marker to identify melting when it occurs

crystalline state in the solid phase. It does so at a significant rate for silicon in the temperature range above about 400°C. Bagley and Chen predict that for silicon the melting point of the amorphous phase, T_T, and its enthalpy of melting, $\Delta H_{\ell\alpha}$, will both be about 25 percent below crystalline values. Extremely rapid heating is required to reach T_T in the amorphous state because the solid phase transformation is rapid at elevated temperatures (milliseconds for 2000Å layers at 1000°C) [8].

Baeri, Foti, Poate, Cullis [9] have studied this regime using pulsed electron beams for rapid excitation. Their experiment is illustrated in Figure(5). An arsenic layer served as a marker for melting. It was implanted and oven annealed (in the solid phase to avoid impurity redistribution). An amorphous layer was then formed on half of the sample by phosphorous implantation. These double samples were subjected to 50 nsec electron pulses with pulse energies between 0.42 and 1.3 J/cm^2.

The arsenic depth distributions following 0.65 and 1.1 J/cm^2 pulses are shown on the left side of Figure(6). At 0.65 J/cm^2 the arsenic distributions broaden for both the amorphous and crystalline parts of the sample. The amorphous region shows greater broadening as might be expected if deeper melting has occurred in that region because less energy is required to melt the already disordered silicon. At 1.1 J/cm^2 the broadening is increased for both regions, but the difference is now unmeasurable. Calculated profiles of arsenic are shown on the right side of Figure(6). An enthalpy of melting of 1220 ± 150 J/gm for the amorphous compared with 1790 J/gm for crystalline silicon gives good agreement with experiment.

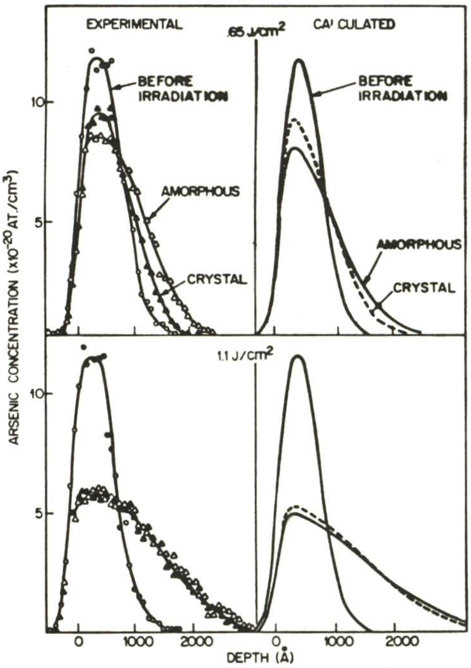

Fig. 6 Arsenic concentration before and following pulsed electron irradiation at two energy densities as measured and calculated [9]

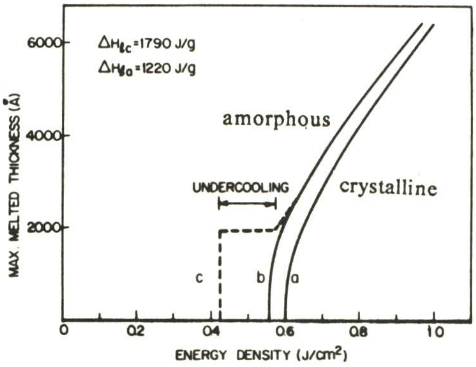

Fig. 7 Calculated maximum melt layer thickness as a function of pulsed electron energy density in Si with a 1900Å amorphous surface layer [9]. The dashed undercooling region assumes T_T=1170K

The calculated melt depth versus energy density for the two regions is shown in Figure(7). The dashed step in the figure illustrates another expectation. If T_T is below T_m, at low enough pulse energy densities, the amorphous layer should all melt before any of the crystalline material melts. In the experiment this region was found below 0.55 J/cm^2. At 0.55 J/cm^2 the originally amorphous layer became single crystal but with defects at the original interface. At 0.5 J/cm^2 a layer approximately 800Å thick regrew epitaxially on the underlying silicon but was heavily twinned. The upper 1000Å was polycrystalline. At this energy density the melted layer is strongly super cooled with respect to T_m and will crystallize extremely rapidly. It has apparently regrown from both the silicon interface and from the free surface. Based on these observations and confirming channeling measurements of the regrown layer, T_T has been estimated to be 1170 ± 100 K. The values of T_T and $\Delta H_{\ell\alpha}$ are both somewhat below the estimates by Bagley and Chen, but with uncertainties that encompass them.

III. Explosive Crystallization

The crystallization from a super-cooled liquid as discussed in Section II for nanosecond electron pulses can also occur in conditions of explosive crystallization. This name refers to the rapid and self-sustaining crystallization of an entire amorphous film after crystallization is initiated at any point of the film as shown in Fig. (8) Initiation can be by a localized heat pulse from a laser, for example. Typical speeds for the propagation of a crystallization front across the film are ≈1 meter/second with crystallization sustained over distances of many centimeters [10]. The field of explosive crystallization has a long history, with a recent resurgence of interest in the 1970s with the work of Mineo [10] and others [11].

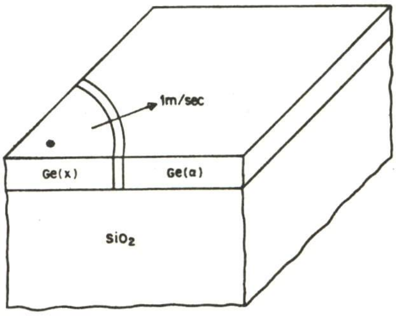

Fig. 8 Schematic illustration of explosive crystallization of an amorphous germanium film on amorphous SiO_2

It is clear that crystallization is sustained by the energy released in the crystallization at the advancing front. The speed of crystallization, however, raises serious questions as to whether it can be taking place in the solid phase [12,13]. Gold et al. [12] have suggested a mechanism of "duplex melting" involving a supercooled liquid. Gilmer and Leamy [13] have considered the question theoretically and concluded that a thin super-cooled molten layer exists at the crystallization boundary. Heat released by crystallization raises the adjacent amorphous material to a temperature above the amorphous melting point but below the melting point of crystalline germanium. Crystallization then occurs rapidly from this super-cooled liquid phase.

To test their conclusion an experiment has been performed on 4μ thick Ge films into which markers of antimony and lead have been implanted [14]. If a liquid layer exists, liquid phase diffusivity of the impurities should result in changes in their depth distribution. The substrate was heated to 310°C and crystallization initiated at a point with an argon ion laser beam.

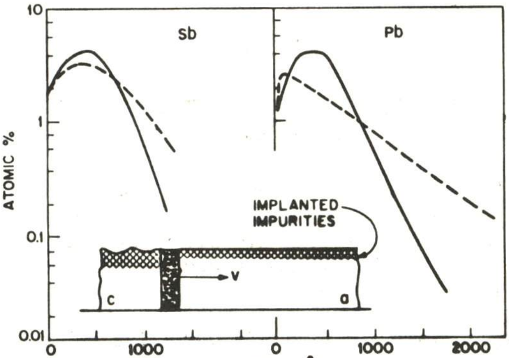

Fig. 9 Depth distributions of Sb and Pb before and after explosive crystallization [14]

Backscattering measurements of the impurity depth distributions before and after the crystallization are shown in Figure (9) Both impurities have spread into the film in confirmation of the molten layer expectation. At a 1 m/sec crystallization front velocity, the extent of the antimony redistribution implies a molten zone width of 200 to 400Å. This is consistent with a predicted width of approximately 1 percent of the film thickness. The depth distribution for lead is different; deeper into the germanium and with a shallower concentration gradient. The sense of this difference is to be expected from the lower segregation coefficient of lead and hence its longer residence time in the melt.

IV. Impurity Incorporation

As has been reported by many authors [15], the rapid solidification of silicon following laser melting results in incorporation of impurities in the final crystal in excess of the equilibrium solid solubility limit. The result can be thought about in terms of solute trapping [16]. Solute atoms that would normally be rejected at the solid-liquid interface do not have time to diffuse away from the solidification front and are trapped in the crystal [16]. The result could be expected to be strongly influenced by the liquid diffusivity of the impurities in comparison with the solidification velocity.

The solidification velocity can be varied in the laser melting regime over an interesting range. Figure 10 is a calculation from Baeri, et al. [17] of the average velocity over the last 1000Å of silicon solidification following ruby laser pulses of 15 and 50 nsec and different energy densities. The maximum depth of melt penetration is also indicated. The shorter pulses require less laser energy to melt a given depth because there has been less time for thermal diffusion into the material. Varying the substrate temperature and hence the thermal conductivity produces yet another means of changing the velocity of regrowth as shown by Cullis et al. [18].

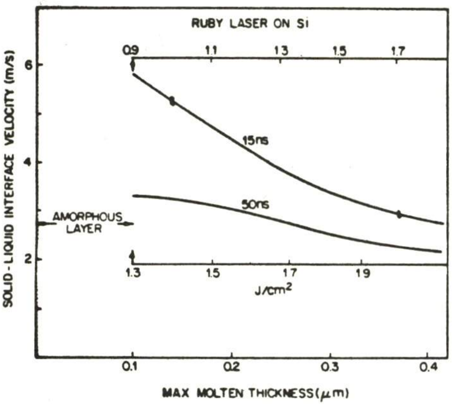

Fig. 10 Calculated interface velocities [17] for regrowth of silicon following 15 and 50 nsec. laser pulses of different energy density: The maximum molten thickness is shown on the bottom scale

The incorporation of different impurities is quite different. Arsenic is an example with a high equilibrium segregation coefficient k=0.3. Depth profiles due to White et al. [19] are shown in Figure 11 before and after laser melting. The broadening of the distribution can be well accounted for by diffusion of arsenic in the transiently melted surface layer with a k′ (nonequilibrium) of 1.0. The concentration also exceeds the equilibrium solid solubility (in this case by a factor of about three).

The case for indium is quite different. In Figure 12 a large part of the indium is shown segregated to the surface, but the amount that is incorporated in the growing crystal (and in substitutional lattice sites) is orders of magnitude more than would have been expected if the growth had occurred near equilibrium, as shown by the lower-line in the figure. White et al. [19], determined that a value of k′ = 0.15 gives a reasonable account of the incorporated impurities.

Baeri et al. [17], have examined the indium case as a function of regrowth velocity. A few of their results are shown in Figure 13. In these depth profiles, regrowth velocity has been varied by laser pulse length and energy density as shown in Figure 10. At the highest velocity, 5.2m/sec, 60 percent of the indium is retained in the crystal while the retained fraction drops to less than 5 percent as the regrowth velocity drops below about 3m/sec. The dependence of k′ on regrowth velocity is given in Figure 14. The velocity is remarkably critical.

The idea of solute trapping can be considered by comparing two times, the time for advance of the crystal front by one layer and the time for impurities in the liquid to diffuse a similar distance. At 4m/sec the crystal advance time for a 2 Å layer distance is 5×10^{-11} sec. For a solid with a liquid diffusivity of 10^{-5}cm^2/sec, the diffusion time for the same distance is 4×10^{-11} sec. These numbers are certainly comparable and might account for the indium result. However, the diffusion coefficient for arsenic is approximately 10^{-4}cm^2/sec and the diffusion time would then be ten times shorter. This simple trapping argument fails to explain the increase in k′ quantitatively. The metallurgy at the interface matters. More careful studies of both the orientation dependence of crystal growth and impurity incorporation and their velocity dependence will be needed to get a satisfactory explanation. The temperature of the

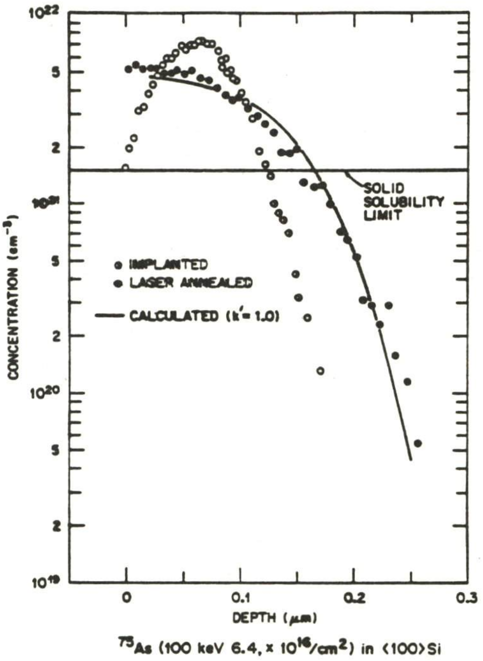

Fig. 11 The distribution of implanted arsenic before and after laser annealing, due to White, et al [20]. The calculated curve assumes a nonequilibrium K′=1.0. The equilibrium solid solubility limit is shown

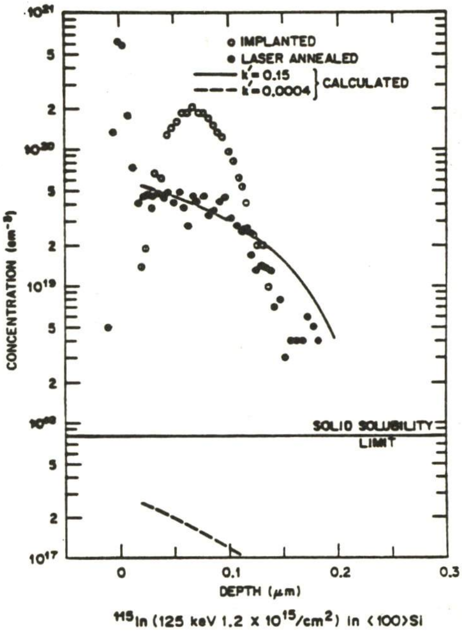

Fig. 12 The distribution of implanted indium before and after laser annealing, due to White, et al [20]. Note the large surface segregation and the fit of the data to a k′=0.15

growing interface would be extremely valuable to know, since the extent of supercooling is influenced by the presence of high impurity concentrations and the chemical nature of the impurities as well. This influence is already strongly evident in the cellular structures observed and attributed to constitutional supercooling for normally low k impurities such as platinum [18], indium [17] and gallium [21].

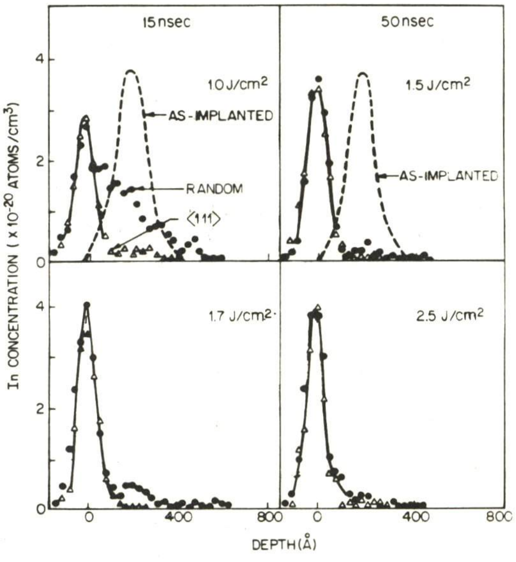

Fig. 13 Experimental depth distributions of indium due to Baeri et al [17] for different regrowth velocities obtained by varying the pulse length and energy density of ruby laser pulses

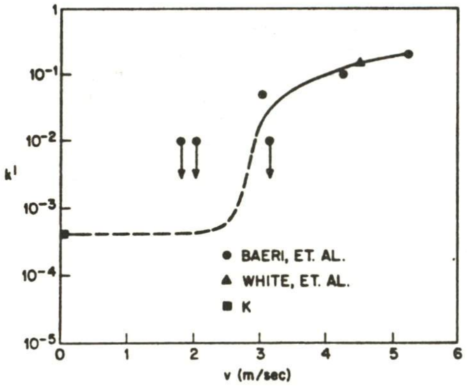

Fig. 14 Nonequilibrium segregation coefficient of indium obtained from experiments at different regrowth velocities

V. The Question of Energy Transfer

As indicated in Section I, the widely accepted view of nanosecond pulsed laser or electron beam processing, "annealing", in semiconductors involves electronic excitation of electrons and holes and rapid equilibration (at least on a nanosecond time scale) of the electrons and holes with lattice vibrations (phonons) of the solid. If the pulse energy density is high enough, the solid melts in a thin layer at the surface and subsequently refreezes. There is broad consistency of this picture with a large body of measurements on impurity redistribution (and its dependence on temperature, impurity concentration, energy density, pulse length and wavelength), the dissolution of precipitates [21], the disappearance [22] (and growth) of dislocations, the formation of polycrystalline or epitaxial single crystal material, the cleaning of surfaces in vacuum [23], and even the formation of amorphous material at extremely high solidification velocities [24].

The measurement of time resolved optical reflectivity provides an independent confirmation of this melting model, as shown in Fig. (15)from Auston et al. [25]. The flat topped pulse of high reflectivity corresponds to reflection from liquid silicon. Its duration, τ, corresponds to the duration of a melted layer at the very surface, since the probe light penetrates into the liquid only ~200Å. The dependence of τ on laser energy density and wavelength and on the absorbing properties of the material (amorphous or crystalline) agrees well with calculations based on the thermal melting model.

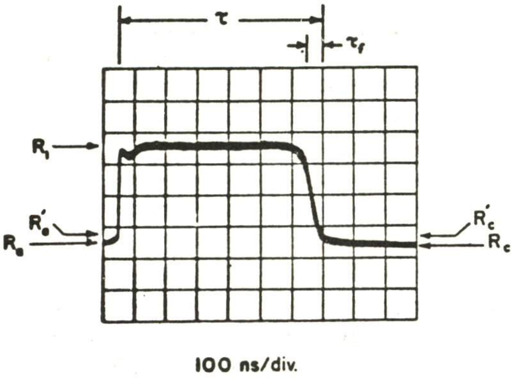

Fig. 15 Transient reflectivity due to Auston et al [25] during and following a 30 nsec. Nd:Glass 532 nm. pulse of 2.75J/cm^2: The marked reflectivities are: amorphous, R_a; crystalline, R_c; liquid, R_l; hot amorphous, R_a'; hot crystalline, R_c'

The melting model has been questioned by Khaibullin et al [26] and rejected by Van Vechten [28] who proposes instead that the electron-hole density generated by the pulsed laser or electron beam is so high that it becomes decoupled from transfer of the excitation to phonons (heat) and can exist out of equilibration with the lattice for tens or even hundreds of nanoseconds. Van Vechten ascribes Auston's observed high reflectivity to reflectance from this plasma whose density is high enough to have a plasma frequency above the probe laser frequency. The crystal growth, impurity incorporation, precipitate dissolution, etc. are all ascribed to processes driven by the high electron-hole density which provides so many broken bonds that the material is fluid-like, but the atoms are cool.

Calculations by Yoffa [28] have failed to support a picture of long delayed equilibration of electrons with the lattice. In fact, they indicate electron-phonon coupling times even at very high carrier densities which are the order of 10^{-10} sec. Recent measurements by Nathan et al [29] have been carried out to measure the reflectivity at two laser frequencies to see if an expected dependence on the plasma density would appear. Fig. 16 shows the published results. Within the scatter of the measurements there is no difference, although the high reflectivity would be expected to persist considerably longer for the lower frequency (longer wavelength) probe light which requires a lower plasma density for high reflectivity. Equality in duration of observed high reflectivity would be expected for a melting model, which these data support.

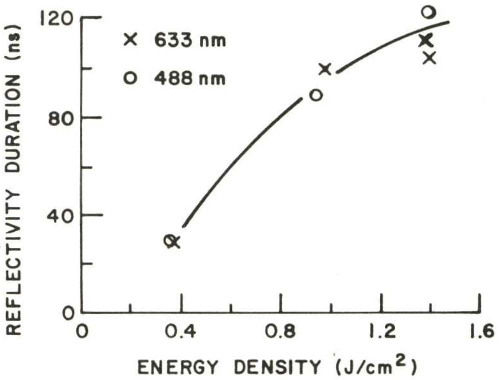

Fig. 16 Duration of reflectivities measured by Nathan et al [30] using probe lasers of two different wavelengths with heating pulses in all cases at 530 nm

Even more recently, Lo and Compaan [30] have reported Raman scattering studies which are designed to measure the temperature of the material directly through the relative intensity of the Stokes/anti-Stokes lines of the LO phonon at 520 cm^{-1}. On crystalline silicon they find temperature rises of only a few hundred degrees centigrade at laser heating energy densities which produce the high reflectivity regime that has been associated with melting. These results are shown in Fig. 17. For ion implantation amorphized silicon these authors report observations of a crystalline Raman signal that develops during the high reflectivity phase of the pulse [31]. These Raman results are provocative and apparently inconsistent with the melting model. They may be consistent with Van Vechten's plasma model. Such measurements are extremely difficult and confirmation of these initial findings is clearly very important.

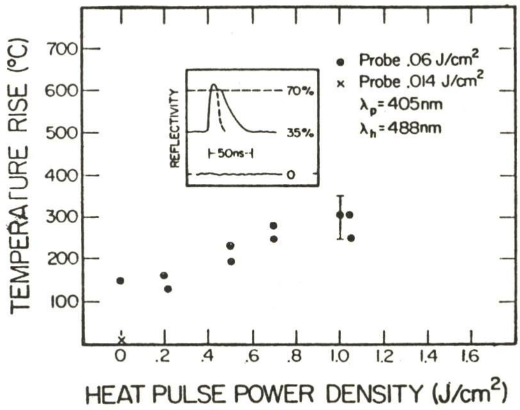

Fig. 17 Temperature rise determined from Stokes/antiStokes ratios in Raman scattering probed at 405 nm. with heating pulses at 488 nm. Due to Lo and Compaan [31]

Other time resolved studies are being made by Murakami et al. [32] measuring reflectivity in response to picosecond laser pulses and by Yamada et al. [33] who are studying conductivity and reflectivity transients in silicon on sapphire. Reports of both of these will be included in the proceedings of the Kyoto conference.

The question of energy transfer following intense excitation is of fundamental significance. New experiments that provide more detailed understanding of the time scale and energy density dependence for equilibrium of carriers with the lattice will be needed to test existing theoretical expectations.

References

1) See Laser and Electron Beam Processing of Materials, Editors: C. W. White and P. S. Peercy, Academic Press, 1980, New York.

2) M. vanAllmen ; Laser and Electron Beam Processing of Materials, C. W. White and P. S. Peercy, eds., Academic Press (1980), p. 6.

3) W. L. Brown in Laser and Electron Beam Processing of Materials, C. W. White and P. S. Peercy, eds., Academic Press (1980), p. 20.

4) A. Lietoila and J. F. Gibbons; Appl. Phys. Lett. 34, 332 (1979).

5) P. Baeri, S. U. Campisano, G. Foti and E. Rimini. J. Appl. Phys. 50, 788 (1979).

6) J. S. Williams, W. L. Brown, G. K. Celler, H. J. Leamy, J. M. Poate, G. A. Rozgonyi and T. T. Sheng: J. Appl. Phys., in press.

7) B. G. Bagley and H. S. Chen : Laser-Solid Interactions and Laser Processing - 1978, S. D. Ferris, H. J. Leamy and J. M. Poate, Eds., Amer. Institute of Physics 1979, New York, p. 97.

8) J. S. Williams, W. L. Brown, H. J. Leamy, J. M. Poate, J. W. Rodgers, D. Rousseau, G. A. Rozgonyi, J. A. Shelnutt and T. T. Sheng; Appl. Phys. Lett. 33, 542 (1978).

9) P. Baeri, G. Foti, J. M. Poate and A. G. Cullis; Phys. Rev. Lett., to be published.

10) A. Mineo, A. Matsuda, T. Kurosu and M.Kikuchi: Solid State Comm. 13, 329 (1973).

11) T. Takamori, R. Messier and R. Roy; Appl. Phys. Lett. 20, 201 (1972); T. Takamori, R. Messier and R. Roy: J. Materials Science 8, 1809 (1973); R. Messier, T. Takamori, and R. Roy: Solid State Comm. 16, 311 (1974); A. Matsuda, A. Mineo, T. Kurosu, and M. Kikuchi; Solid State Comm. 13, 1165 (1973); M. Kikuchi, A. Matsuda, T. Kurosu, A. Mineo and M. J. Callanan: Solid State Comm. 14, 731 (1974).

12) R. B. Gold, J. F. Gibbons, T. J. Magee, J. Peng, R. Ormond, V. R. Deline and C. A. Evans; Jr. in Laser and Electron Beam Processing of Materials, C. W. White and P. S. Peercy, eds., Academic Press (1980), p. 221.

13) G. H. Gilmer and H. J. Leamy : Laser and Electron Beam Processing of Materials, C. W. White and P. S. Peercy, eds., Academic Press (1980), p. 227.

14) H. J. Leamy, W. L. Brown, G. K. Celler, G. Foti, G. H. Gilmer and J. C. C. Fan; Appl. Phys. Lett., to be published.

15) See for example J. C. Bean, H. J. Leamy, J. M. Poate and G. K. Celler : Laser Solid Interactions and Laser Processing, Boston (1978) (AIP Conf. Proc. 50) Ed. by S. D. Ferris, H. J. Leamy and J. M. Poate, p. 487; C. W. White, S. R. Wilson, B. R. Appleton, F. W. Young, Jr. and J. Narayan ; Laser and Electron Beam Processing of Materials, C. W. White and P. S. Peercy, eds., Academic Press (1980), p. 111; E. Fogarassy, R. Stuck, J. J. and A. Grob and P. Siffert : Laser and Electron Beam Processing of Materials, C. W. White and P. S. Peercy, eds., Academic Press (1980), p. 117.

16) K. A. Jackson and H. J. Leamy in Laser Solid Interactions and Laser Processing, Boston (1978) (AIP Conf. Proc. 50) Ed. by S. D. Ferris, H. J. Leamy and J. M. Poate, p. 103; J. W. Cahn, S. R. Coriell and W. J. Boettinger in Laser and Electron Beam Processing of Materials, C. W. White and P. S. Peercy, eds., Academic Press (1980), p. 89; K. A. Jackson, G. H. Gilmer and H. J. Leamy in Laser and Electron Beam Processing of Materials, C. W. White and P. S. Peercy, eds., Academic Press (1980), p. 104.

17) P. Baeri, J. M. Poate, S. U. Campisano, G. Foti, E. Rimini and A. G. Cullis; Appl. Phys. Lett., to be published.

18) A. G. Cullis, H. C. Webber, J. M. Poate and A. L. Simons; Appl. Phys. Lett., 36, 320 (1980).

19) C. W. White, S. R. Wilson, B. R. Appleton and F. W. Young, Jr.; J. Appl. Phys. 51, 738 (1980).

20) C. W. White, S. R. Wilson, B. R. Appleton and J. Narayan ; Laser and Electron Beam Processing of Materials, C. W. White and P. S. Peercy, eds., Academic Press (1980), p. 124.

21) J. Narayan and C. W. White in Laser and Electron Beam Processing of Materials, C. W. White and P. S. Peercy, eds., Academic Press (1980), p. 65.

22) J. Narayan and F. W. Young, Jr.: Appl. Phys. Lett. 35, 330 (1979).

23) D. M. Zehner, C. W. White, C. W. Ownby and W. H. Christie : Laser and Electron Beam Processing of Materials, C. W. White and P. S. Peercy, eds., Academic Press (1980), p. 201; P. L. Cowan and J. A. Golovchenko, J. Vac. Sci. and Tech., in press.

24) P. L. Liu, R. Yen, N. Bloembergen and R. T. Hodgson in Laser and Electron Beam Processing of Materials, C. W. White and P. S. Peercy, eds., Academic Press (1980), p. 156.

25) D. H. Auston, C. M. Surko, T. N. C. Venkatesan, R. E. Slusher and J. A. Golovchenko: Appl. Phys. Lett. 33, 437 (1978); Appl. Phys. Lett. 34, 635 (1979); AIP Conf. Proc. of Laser-Solid Interactions and Laser Processing, eds. S. D. Ferris, H. J. Leamy and J. M. Poate (1979), p. 11.

26) I. B. Khaibullin, E. I. Shtyrkov, M. M. Zaripov, R. M. Bayazitov and Galjautdinov: Radiation Effects 36, 225 (1978).

27) J. A. Van Vechten, R. Tsu and F. W. Saris; Phys. Lett. 74A, 422 (1979); J. A. Van Vechten in Laser and Electron Beam Processing of Materials, C. W. White and P. S. Peercy, eds., Academic Press (1980), p. 53.

28) E. J. Yoffa : Laser and Electron Beam Processing of Materials, C. W. White and P. S. Peercy, eds., Academic Press (1980), p. 59.

29) M. I. Nathan, R. T. Hodgson and E. J. Yoffa; Appl. Phys. Lett. 36, 512 (1980).

30) H. W. Lo and A. Compaan; Phys. Rev. Lett. 44, 1604 (1980).

31) A. Compaan and H. W. Lo; Proc. of Conf. on Defects in Semiconductors, Oiso, Japan (1980).

32) K. Murakami, M. Kawabe, K. Gamo, S. Namba and Y. Aoyagi, : Proc. of 15th Int. Conf. on the Physics of Semiconductors, Kyoto, Japan (1980).

33) M. Yamada, S. Hara, H. Kotani, K. Yamamoto and K. Abe : Proc. of 15th Int. Conf. on the Physics of Semiconductors, Kyoto, Japan (1980).